



ELSEVIER

Available online at [www.sciencedirect.com](http://www.sciencedirect.com)

ScienceDirect

journal homepage: [www.elsevier.com/locate/he](http://www.elsevier.com/locate/he)

## Review Article

# Effect of hydrocarbon fractions, N<sub>2</sub> and CO<sub>2</sub> in feed gas on hydrogen production using sorption enhanced steam reforming: Thermodynamic analysis

Zainab Ibrahim S G Adiya<sup>\*</sup>, Valerie Dupont, Tariq Mahmud

School of Chemical and Process Engineering (SCAPE), The University of Leeds, Leeds LS2 9JT, UK

## ARTICLE INFO

## Article history:

Received 24 March 2017

Received in revised form

8 June 2017

Accepted 21 June 2017

Available online xxx

## Keywords:

Shale gas

Steam reforming

Sorption enhancement

C1–C3 species

N<sub>2</sub>CO<sub>2</sub>

## ABSTRACT

H<sub>2</sub> yield and purity from sorption enhanced steam reforming (SE-SR) are determined by temperature, S:C ratio in use, and feed gas composition in hydrocarbons, N<sub>2</sub> and CO<sub>2</sub>. Gases with high hydrocarbons composition had the highest H<sub>2</sub> yield and purity. The magnitude of sorption enhancement effects compared to conventional steam reforming (C-SR), i.e. increases in H<sub>2</sub> yield and purity, and drop in CH<sub>4</sub> yield were remarkably insensitive to alkane (C1–C3) and CO<sub>2</sub> content (0.1–10 vol%), with only N<sub>2</sub> content (0.4–70 vol%) having a minor effect. Although the presence of inert (N<sub>2</sub>) decreases the partial pressure of the reactants which is beneficial in steam reforming, high inert contents increase the energetic cost of operating the reforming plants. The aim of the study is to investigate and demonstrate the effect of actual shale gas composition in the SE-SR process, with varied hydrocarbon fractions, CO<sub>2</sub> and N<sub>2</sub> in the feedstock.

© 2017 The Authors. Published by Elsevier Ltd on behalf of Hydrogen Energy Publications LLC. This is an open access article under the CC BY license (<http://creativecommons.org/licenses/by/4.0/>).

## Contents

Introduction .....	00
Process background .....	00
Methodology of the thermodynamic equilibrium calculation .....	00
Results and discussion .....	00
Effect of varying composition in feedstock on SE-SR process outputs .....	00
H <sub>2</sub> yield, H <sub>2</sub> purity and selectivity to calcium carbonate product .....	00
Magnitude of sorption enhancement effects due to hydrocarbon content in feed gas .....	00
Magnitude of sorption enhancement effects due to N <sub>2</sub> and CO <sub>2</sub> content in the feed gas .....	00
Enhancement effects of SE-SR vs. C-SR for SG1-4 .....	00

<sup>\*</sup> Corresponding author.

E-mail address: [xeeadiya@yahoo.com](mailto:xeeadiya@yahoo.com) (Z.I. S G Adiya).

<http://dx.doi.org/10.1016/j.ijhydene.2017.06.169>

0360-3199/© 2017 The Authors. Published by Elsevier Ltd on behalf of Hydrogen Energy Publications LLC. This is an open access article under the CC BY license (<http://creativecommons.org/licenses/by/4.0/>).

Please cite this article in press as: S G Adiya ZI, et al., Effect of hydrocarbon fractions, N<sub>2</sub> and CO<sub>2</sub> in feed gas on hydrogen production using sorption enhanced steam reforming: Thermodynamic analysis, International Journal of Hydrogen Energy (2017), <http://dx.doi.org/10.1016/j.ijhydene.2017.06.169>

Effect of temperature on SE-SR process output .....	00
Effect of steam to carbon ratio on process outputs .....	00
Effect of inert bed materials, hydrocarbon fractions, inert N <sub>2</sub> and CO <sub>2</sub> and on enthalpy balance .....	00
Effect of inert bed materials on energy balance .....	00
Effect of hydrocarbon fractions on enthalpy balance .....	00
Effect of N <sub>2</sub> and CO <sub>2</sub> content in the feed gas on enthalpy balance .....	00
Conclusion and final remarks .....	00
Acknowledgement .....	00
Supplementary data .....	00
References .....	00

## Introduction

All hydrocarbon fuels, be them conventional natural gases, shale gases, i.e., gases trapped in shale formations, associated gases or ‘flare’ gas produced at refineries, can be used in hydrogen (H<sub>2</sub>) production [1]. Natural gas has been recently publicised as a bridge fuel to a low carbon future due to its favourable H<sub>2</sub>-to-carbon ratio and newly developed technologies allowing to tap enormous amount of shale gas reserves worldwide that were previously inaccessible [2,3]. With the new found abundance of natural gas that is readily available and can be supplied at a competitive cost, natural gas will remain a very significant contributor to the energy mix [3,4]. A boom in shale gas production [5] in the world foresees that gas will remain the main feedstock of steam reforming in the near term, in contrast to naphtha, which is declining due to high availability of natural gas [5,6]. The 2017 Annual Energy Outlook projected that the U.S (world largest producer of shale gas) natural gas production will increase (an estimate of nearly 4% annual average) as it has since 2005 [7]. An enormous amount of this projected increase is expected from shale gas extraction [7–9]. Additional techniques of natural gas consumption are also desirable (owing to its newfound abundance), including methodologies for proficient H<sub>2</sub> production in small scale, ‘distributed fashion at a point of use’. Distributed H<sub>2</sub> production will assist in overwhelming one of the key ‘barriers to the implementation of a so called H<sub>2</sub> economy’ (the absence of large scale delivery infrastructure) [3].

H<sub>2</sub> is a very important element with a vast range of application and use [10,11]. It is at present being utilised in many industries, from petroleum refining and chemicals production (NH<sub>3</sub>, HCl) to food (production of hydrogenated vegetable oils such as butter and margarine), metallurgical, glass (to form the rim on glass) as well as power and electronics industries (rotor coolant for turbo generators) [10]. H<sub>2</sub> is mainly used as a chemical feedstock in the production of, for example, petrochemicals and ammonia (Haber-Bosch process) in synthetic fertilizer industries [10,12,13]. Ammonia production individually represents the H<sub>2</sub> largest demand, consuming about 50% of all the H<sub>2</sub> produced in the world [10,14,15]. Significant amounts of H<sub>2</sub> are also consumed during hydroprocessing (hydrotreating and hydrocracking processes) in refineries. Interestingly 84% of a typical

hydrocracker operating costs arise from H<sub>2</sub> alone (15% utilities and 1% catalyst) [16]. World-wide consumption of merchant H<sub>2</sub> used for petroleum refining has been projected to rise 5.3% annually through 2018 [17]. It has also been projected that H<sub>2</sub> demand in the world chemical manufacturing market will increase to 4.8% per year to 38.8 billion cubic meters in 2018. Demand in other global markets, totalled, is predicted to rise 4.2% per year to 31.7 billion cubic meters in 2018 [17]. H<sub>2</sub> is also used as raw fuel for fuel cells, which have the power to produce electricity without the air emissions associated with conventional combustion devices used as transport engines or stationary gas turbines. Low temperature fuel cells have increased the significance of H<sub>2</sub> because they need a continuous supply of pure H<sub>2</sub> and air [18]. Furthermore, H<sub>2</sub> gas also has the highest higher heating value of any fuel (120.2 MJ kg<sup>-1</sup>) and the only by product of its combustion is water without any greenhouse or pollutant emission such as CO<sub>2</sub> in the environments [1].

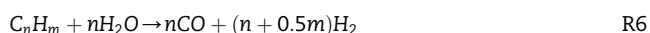
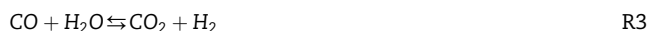
Conventional steam reforming (C-SR) is the most recognised and commonly used process to produce H<sub>2</sub> on a large scale [19]. Approximately 90% of the world’s overall H<sub>2</sub> production is by C-SR of fossils fuels [14,19,20]. The technology has also dominated syngas production for a good 70 years. Even though efforts have been endlessly made to enhance the process by improving catalyst activity and operating conditions including heat transfer to reach a better performance, an inevitable hitch of the process is its intensive energy requirement [21]. Furthermore, the process has caused many environmental problems such as increase in global warming gases concentration in the atmosphere (especially CO<sub>2</sub>). Presently, ‘the CO<sub>2</sub> increasing rate is about 8 billion tons per year’, thus making the reduction of such gases, especially CO<sub>2</sub>, extremely important [22]. The sorption enhanced steam reforming (SE-SR) process aims to address both problems. Detail background/description of the processes is given in the next section.

Although numerous thermodynamic studies have been carried on the Sorption Enhanced steam reforming process using various feedstocks and operating conditions such as oxygenated hydrocarbons [23–25], urea [26], pure methane [3,27,28], pure propane [29] and bio-oil/biogas [30] including coke oven gas but coupled with chemical looping such as Shaojun et al [31], none of the studies looked into the range of mixtures of hydrocarbon gases present in shale gas as SR feedstock, not to mention the effect that significant amount of inert gases can have on the steam reforming process.

This studies aim to investigate the thermodynamics of shale gas as it comes out of the ground with higher hydrocarbons such as  $C_2H_6$  and  $C_3H_8$  in addition to  $CH_4$  (main hydrocarbon component), an inert ( $N_2$ ) and impurity ( $CO_2$ ) [4]. In addition the effect of coupling Conventional steam reforming (C-SR) with - the Sorption Enhancement (SE) process is investigated as well as identifying the optimum operating condition of the SE-SR process when operating with shale gases feedstocks. Detail description of processes with schematic can be found in S G Adiya et al. [32].

## Process background

The term conventional steam reforming refers to a catalytic reaction (metallic nickel being the most common catalyst) between a volatile organic fuel which may be non-oxygenated, such as methane, natural gas [1], or oxygenated, such as bio-oil [33,34], and steam. The main steps in the industrial process are represented by Reactions R1, i.e. the generation of syngas ( $H_2$ ,  $CO$ ), with co-product  $CO_2$  (R2) at high temperature 800–950 °C and medium pressure 20–35 atm [20,35–37]. The syngas may be further reacted at lower temperature 200–400 °C [20,37–39] to maximise  $H_2$  generation, through the reaction of water gas shift ‘WGS’ (R3). Taken together the overall process SR R1 and WGS R3 reaction results into R2, the complete steam methane reforming reaction. Even though the WGS is exothermic, the global energy requirement of the process is significantly endothermic [20], necessitating an external source of energy. It is worth nothing that thermal decomposition of the fuel produces C and  $H_2$  (R4), so, although R4 generates  $H_2$ , it is undesirable as it deactivates the catalyst by carbon deposition as well as decreases the yield of  $H_2$  compared to steam reforming. A desirable by-production of  $H_2$  comes from dry reforming (R5) because two molecules ( $CH_4$  and  $CO_2$ ) that contribute to greenhouse effect significantly are converted into valuable products ( $H_2$  and  $CO$ ). Natural gas, whose main component is methane but also features significant amounts of C > 1 species (hydrocarbons with carbon number higher than one), also undergo steam reforming via general reaction R6 (like ethane (R7) and propane (R8)), followed by the water gas shift reaction R3. Studies on dry reforming R5 occurring concurrently with SR are limited/not available.

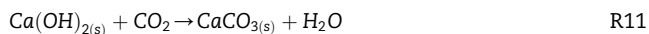


Other side reactions also take part during steam reforming process, for example, CO disproportionation, a.k.a. Boudouard reaction (R9), exothermic and requiring low temperatures (<400 °C) and reverse Boudouard (R9<sub>b</sub>) reaction, endothermic and common at steam reforming temperatures. Methanation reactions (R1<sub>b</sub> and R2<sub>b</sub>) where subscript ‘b’ denotes reverse direction), which are the reverse steam reforming and the reverse water gas shift reaction (R3<sub>b</sub>), are also possible reactions in steam reforming processes. The equilibrium of methanation vs. steam reforming is very temperature and pressure dependent, the latter prevailing at higher temperatures and lower pressures.

Separation/purification marks the end of the process (C-SR). This step is downstream of the WGS. Various techniques are available that can be used to achieve the separation process. Pressure swing absorption (PSA), membranes, and cryogenics are the most commonly used techniques for syngas separation [20,40,41]. PSA separation techniques are technically mature technologies that can provide high degrees of end  $H_2$  purity (up to > 99%). However, membrane technology is a promising and developing technology but also has the ability to generate high purity  $H_2$  (>99%) [20]. Chemical absorption for example  $CO_2$  scrubbing using methyldiethanolamine (MDEA), monoethanolamine (MEA), activated methyldiethanolamine (aMDEA) are also used for separation but purity of  $H_2$  is less than with PSA, membrane or cryogenics [42]. Detailed overview on membrane separation and chemical absorption can be found in Adhikari and Fernando [43] and Yildirim et al. [42] respectively. It is worth noting that the final separation step is not covered in the present study.

One major concept for  $CO_2$  emission reduction is  $CO_2$  sequestration, in which  $CO_2$  is absorbed in the emission source, preventing it emission into the atmosphere. A solid  $CO_2$  sorbent is the backbone of this promising technology [44]. The role of  $CO_2$  sorbent can be performed cheaply by the abundant calcium oxide (commonly known as quicklime or burned lime) [1], or as the active component in dolomite, in which case,  $CO_2$  capture is represented by R10 or R11 depending on its hydration state. Calcium oxide is also the most frequently used sorbent in the globe [1]. Other available and suitable  $CO_2$  sorbents include Double salt (e.g.  $(K_2CO_3)(2KHCO_3)(MgCO_3)(MgO)_x \cdot xH_2O$ ), hydrotalcites (e.g.  $Mg_6Al_2(OH)_{16}(CO)_3 \times 4H_2O/K_2CO_3$ ), Li metal oxide (e.g.  $Li_4SiO_4$ ) and supported sorbents (e.g. CaO on cobalt superior micro-powder) [45–49]. It is of utmost importance for the sorbent to have a high selectivity and adsorption capacity at operating temperature and pressure. The loss of absorption capacity during cyclic operation is primarily caused by sintering of the sorbent. This include change in pore shape of the particle and agglomeration of small particle size. Thus, causing the carbonation process (R10 or R11) to occur just on the external surface of the sorbent [50–52] rather than the full material's volume. This undesirable phenomenon can be prevented by improving the stability of the material by incorporating an inert support material to the sorbent [44] such as Aluminium oxide ( $Al_2O_3$ ) [53], Silica oxide ( $SiO_2$ ) [54], Yttrium oxide ( $Y_2O_3$ ) [55], titanium oxide ( $TiO_2$ ) [56], and Zirconium oxide ( $ZrO_2$ ) [57]. In addition, an ideal sorbent should have good and steady

adsorption ability of CO<sub>2</sub> after repeated adsorption and desorption cycles, including good mechanical strength of adsorbent particles after cyclic exposure to high pressure streams [45,58].



The main aim of SE-SR in packed bed reactor configuration is to improve the well-known C-SR process [59]. In other words, all the three basic steps in the conventional method i.e. steam reforming, WGS and separation step are conducted simultaneously in a single reactor vessel in the presence of catalyst and a solid CO<sub>2</sub> sorbent. The process (SE-SR) is well researched, with pilot scale plants (capacity ranging from 2 to 20 MW) built in Sweden, Australia, and Germany for syngas production [60–62]. In fact H<sub>2</sub> production from hydrocarbon in the presence of CaO<sub>(s)</sub> sorbent reportedly took place as early as 1868 [1,63]. A patent for H<sub>2</sub> production using SE-SR process was issued in 1933 [1,64]. The process is operated in cyclic reforming/calcining mode achieved with alternating feed flows in two packed bed reactors. Alternatively, circulating bed materials moving between reformer (fuel-steam reactor) and calciner (air reactor) can be used with two fluidized bed reactors, each operating in continuous flow. Either way the reforming reactor generates the syngas while the calcination reactor performs the CO<sub>2</sub> sorbent regeneration. While it is possible to conduct reforming and calcination semi-batch wise in a single packed bed reactor vessel, causing intermittent H<sub>2</sub> production, it would be more attractive to operate in at least two packed bed reactor vessels [1,63], therefore making the process cyclic with continuous H<sub>2</sub> production and CO<sub>2</sub> capture.

The highly exothermic nature of the carbonation reaction (R10 or R11), means heat is required to regenerate the sorbent

temperatures of about 723–873 K compared to the C-SR process operating condition above 1073 [1,26,46,65]. In addition, the process has the potential to reduce separation/purification steps and extent [45,58], as well as generating pure CO<sub>2</sub> that becomes suitable for subsequent use or sequestration during the sorbent calcination step [45,58,66]. Fig. 1 illustrates the advantages in infrastructure and operational savings that SE-SR may have over C-SR via the elimination of the separate WGS stage and the reduced requirement for the PSA. The CO<sub>2</sub>-rich gas generated during calcination (step 2 of SE-SR, Fig. 1) could potentially be used to run a gas turbine.

## Methodology of the thermodynamic equilibrium calculation

Thermodynamic equilibrium calculation was performed based on minimisation of Gibbs free energy using the CEA software by National Aeronautics and Space Administration (NASA) [67]. The calculation is based on a Newton Raphson iteration procedure [67]. All reactants (CH<sub>4</sub>, C<sub>2</sub>H<sub>6</sub>, C<sub>3</sub>H<sub>8</sub>, N<sub>2</sub>, CO<sub>2</sub>, H<sub>2</sub>O) were considered at equilibrium in the gas-water-Ca based CO<sub>2</sub> sorbent system in addition to H<sub>2</sub>, CO, C<sub>(s)</sub>, NH<sub>3</sub> and Ca containing solid species CaO<sub>(s)</sub> and Ca(OH)<sub>2(s)</sub> for the SE-SR process, with CaCO<sub>3(s)</sub> as additional product. Other related species for example C<sub>4</sub>H<sub>2</sub>, C<sub>4</sub>H<sub>6</sub>, C<sub>4</sub>N<sub>2</sub>, CH<sub>2</sub>, CH<sub>3</sub>, CH<sub>2</sub>OH, C<sub>2</sub>H<sub>4</sub>, C<sub>2</sub>H<sub>5</sub>, CCN, CNC, CN and CH<sub>3</sub>COOH were also considered in the equilibrium calculations however, their equilibrium molar fractions were less than 5 × 10<sup>-6</sup>, thus, neglected.

Outputs of the materials balances were given in terms of H<sub>2</sub> yield as mass percentage of the fuel gas, as well as H<sub>2</sub> purity and selectivity of carbon containing products to calcium carbonate.

With shale gases consisting in X, Y and Z mol % of the alkanes CH<sub>4</sub>, C<sub>2</sub>H<sub>6</sub> and C<sub>3</sub>H<sub>8</sub>, T mol% of CO<sub>2</sub> and I mol % of N<sub>2</sub>, the absolute maxima of H<sub>2</sub> yield, H<sub>2</sub> and CO<sub>2</sub> or CaCO<sub>3</sub> products could be expressed as:

$$\text{Max H}_2 \text{ yield wt\%} = 100 \times \frac{2.02(2n_{\text{SG}} + 0.5m_{\text{SG}})}{12.01n_{\text{SG}} + 1.01m_{\text{SG}} + (44.01T/100) + (28.02I/100)} \quad (1)$$

back to CaO (R10<sub>b</sub> or R11<sub>b</sub>). Thus, once the sorbent is nearly saturated with CO<sub>2</sub>, it is regenerated in situ by temperature (calcination) swing adsorption principle, making the CO<sub>2</sub> sorbent useable again [1,26]. When using CaO as the sorbent, calcination is required as the chemical bonds of the carbonate require severing to release the previously captured CO<sub>2</sub>.

As the CO<sub>2</sub> is captured on a Ca-based sorbent as CaCO<sub>3(s)</sub>, the equilibrium of the H<sub>2</sub> producing process is shifted towards the right, first via enhanced water gas shift reaction, and then, by knock on effect due to drop in CO reactant, via enhanced steam reforming reaction, increasing fuel/feedstocks conversion. Consequently, better H<sub>2</sub> yield and purity are obtained at

where the hydrocarbon content in the shale gas is defined by the molar formula C<sub>n<sub>SG</sub></sub>H<sub>m<sub>SG</sub></sub> with

$$n_{\text{SG}} = \frac{X + 2Y + 3Z}{100} \quad (2)$$

and

$$m_{\text{SG}} = \frac{4X + 6Y + 8Z}{100} \quad (3)$$

Substituting Eqs 2 & 3 into Eq. 1 and simplifying, we obtain Eq. 4 as function of X, Y, Z, T and I

$$\text{Max H}_2 \text{ yield wt\%} = 100 \times \frac{2.02(4X + 7Y + 10Z)}{16.05X + 30.08Y + 44.11Z + 44.01T + 28.02I} \quad (4)$$

$H_2$  purity in the reformat gas for the SG mixtures was defined according to Eq. (5):

$$H_2 \text{ purity} = 100 \times \frac{\text{moles } H_2}{\text{moles all dry gases}} \quad (5)$$

Enhancement effects of SE-SR over C-SR are measured by using Eqs. (6)–(8):

$$\begin{aligned} \text{Percent increase in } H_2 \text{ yield} &= 100 \times (H_2 \text{ yield SE} - SR \\ &\quad - H_2 \text{ yield C} - SR) / H_2 \text{ yield C} \\ &\quad - SR \end{aligned} \quad (6)$$

$$\begin{aligned} \text{Percent increase in } H_2 \text{ purity} &= 100 \times (H_2 \text{ purity SE} - SR \\ &\quad - H_2 \text{ purity C} - SR) \\ &\quad \times / H_2 \text{ purity C} - SR \end{aligned} \quad (7)$$

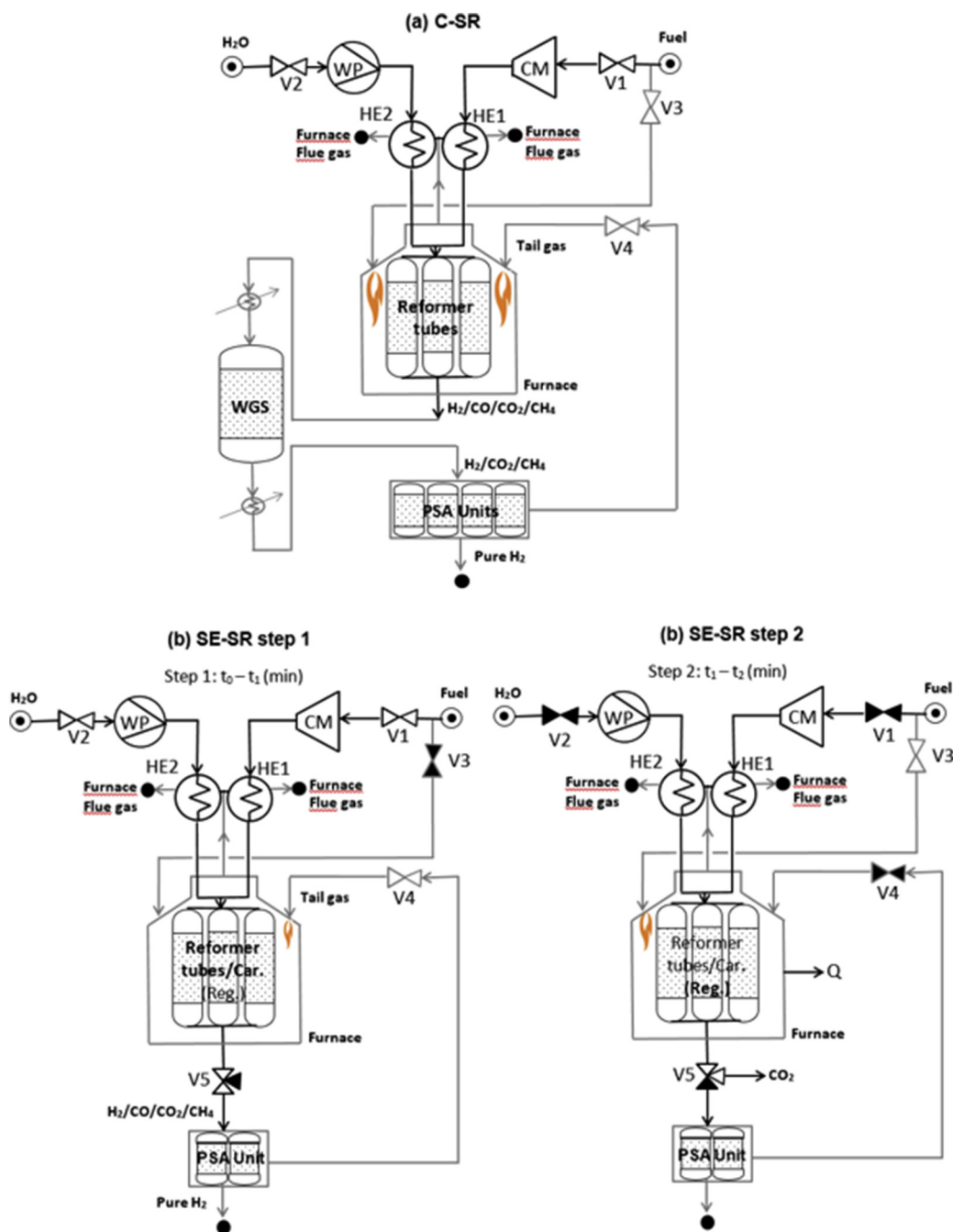


Fig. 1 – Schematic description of (a) C-SR and (b) Steps 1 & 2 of SE-SR using packed bed reactor configuration. Units in grey colour are not covered in our calculation. Blacked out valve symbols (if any) represent closed to flow. Size of flames in furnace are commensurate to heat input from relevant combustible flow (fresh fuel vs. separation unit tail gas).

$$\begin{aligned} \text{Percent drop in CH}_4 \text{ yield} &= 100 \times (\text{CH}_4 \text{ yield C} - \text{SR} \\ &\quad - \text{CH}_4 \text{ yield SE} - \text{SR}) / \text{H}_2 \text{ yield C} \\ &\quad - \text{SR} \end{aligned} \quad (8)$$

The thermodynamic properties (specific heats, enthalpies, entropies) for the initial feed mixture and the equilibrium mixture were from McBride et al. [67]. The National Institute of Standards and Technology (NIST) database and Aspen Plus software's RGibbs model reactor with Ideal and Peng-Robinson properties calculation methods were also used for results verification. The later was conducted at S:C ratio of 3 only. The selected feedstock model composition was based on values found in the literature [68]. Both compositions are actual shale gas composition from the United States [68]. Shale gas termed 'SG1' is from a Marcellus shale which lies in western Pennsylvania, Ohio and West Virginia. The gas composition differs across the field, becomes richer from east to west. Shale gases termed 'SG2', 'SG3' and 'SG4' are from Antrim shale (a shallow shale) in Michigan, U.S. The Antrim shale is unique due to the fact that its gas is predominately biogenic (methane is generated as a by-product of bacterial consumption of organic material in the shale) [68]. Full details on the gases can be found on Bullin and Krouskop [68]. In addition, shale gas termed 'SG1' was chosen because it represents a typical composition of natural gas, containing roughly up to 80% of methane with the remainder made up of higher hydrocarbons (>C3), CO<sub>2</sub> and inert gas [69], representing a mixture rich in ethane and propane. SG1 and SG2 can also represent typical composition of natural gases from Nigeria [70] and UK North sea [71], containing up to 80% methane and Lacq France natural gas containing up to 70% methane [71] respectively. SG3 and SG4 compositions correspond to typical composition of gases with relatively low hydrocarbon and high inert (N<sub>2</sub>) content. The latter will also help in assessing the effect of inert gases in H<sub>2</sub> production. Conditions at equilibrium were provided on the basis of moles of each hydrocarbon gas input (CH<sub>4</sub>, C<sub>2</sub>H<sub>6</sub>, C<sub>3</sub>H<sub>8</sub>), as represented by content in higher hydrocarbon and inert (N<sub>2</sub>) as well as CO<sub>2</sub> in the various gases, with methane always being the main hydrocarbon component, the molar steam to carbon ratio (S:C), as well as system temperature and pressure.

The authors applied their own post processing procedures allowing the calculations of reactants conversions, molar yields of product, and enthalpy balances, including the enthalpy terms associated with bringing to the reaction temperature the reactants from initial room temperature of 298 K and natural phase of feed (gas, liquid water, solid sorbent (CaO<sub>(s)</sub>)). Additional enthalpy terms associated with regeneration of the sorbent were also incorporated in the energy balance calculation. A carbon balance was used to facilitate the calculation of the equilibrium total moles produced for the initial mixture chosen ('N<sub>eq</sub>') and derive products yields and reactants conversions 'X<sub>i</sub>' as shown in Adiya et al. [32].

In the presence of sufficient CaO<sub>(s)</sub> sorbent and steam, maximum H<sub>2</sub> purity for SG1, which contains negligible N<sub>2</sub> (Eq. (5)), could reach 100% as all the hydrocarbon feed content converts to CO<sub>2</sub> and H<sub>2</sub> via steam reforming, with all CO<sub>2</sub> product and feed becoming CaCO<sub>3(s)</sub> carbonate. The latter

would be concurrent with maximum H<sub>2</sub> yield. However, 100% H<sub>2</sub> purity for SG1 could potentially also be attained via 100% conversion through the thermal decomposition reaction, which generates C<sub>(s)</sub> and H<sub>2</sub>, whilst the sorbent would capture the little CO<sub>2</sub> originally present in the SG feed. In this case the H<sub>2</sub> yield would be half the maximum corresponding to just H<sub>2</sub> and CaCO<sub>3(s)</sub> products, because the H<sub>2</sub> content from the water co-reactant would not have been used. For this reason, H<sub>2</sub> purity is considered a secondary output behind H<sub>2</sub> yield. Table 1 displays both the maximum theoretical (stoichiometric) H<sub>2</sub> yields for each shale gas and the H<sub>2</sub> purity values associated with these maxima, assuming the C-SR process and the SE-SR process. In the results section, equilibrium outputs can then be compared with these maxima to assess which conditions were optimum for highest H<sub>2</sub> yield, purity, and energy demand.

As in Adiya et al. [32], the thermal efficiency of the process is assessed here via the 'Δ H ratio'. 'Δ H ratio' is the enthalpy of generating 1 mol of H<sub>2</sub> via the equilibrium process considered (e.g. C-SR or SE-SR), divided by that gained from reacting this H<sub>2</sub> with oxygen, representing its final use in a fuel cell or combustion process [26]. Δ H ratio greater than one (>1) corresponds to a non-efficient process while Δ H ratio <1 is a proficient process and potentially economic from energy perspective. The farther Δ H ratio is from one, the more proficient and feasible the process should be considered. As a measure of theoretical thermal efficiency, Δ H ratio allows comparing between feedstocks for a same process, or between different processes with the same feedstock, based on the same outcome of 1 mol of H<sub>2</sub> produced. Calculations were made based on the enthalpy terms equations defined as in Adiya et al. [32]. For each process, generally two terms were calculated, the change in physical transformations (sensible and latent enthalpy changes for all the species) due to heating and cooling, and the change in reaction enthalpy (isothermal). Regeneration of the Ca-sorbent was assumed to take place at 1170 K, otherwise reforming reactions had given temperatures within a wide range investigated.

For the individual reactants enthalpy change terms, the subscript '1' denoted 'reaction process 1', i.e., the first time step of the cyclic reforming process under consideration (steam reforming and carbonation), and the subscript '2' was

**Table 1 – Composition in mol % for shale gases SG1-4 used in the simulation [68], maximum H<sub>2</sub> yield (Eq. (4)) and corresponding H<sub>2</sub> purity (Eq. (5)) in conditions of max. H<sub>2</sub> yield (Eq. (4)), assuming C-SR and SE-SR.**

Composition	SG1	SG2	SG3	SG4
X (CH <sub>4</sub> )	79.4	77.5	57.3	27.5
Y (C <sub>2</sub> H <sub>6</sub> )	16.1	4.0	4.9	3.5
Z (C <sub>3</sub> H <sub>8</sub> )	4.0	0.9	1.9	1.0
T (CO <sub>2</sub> )	0.1	3.3	0.0	3.0
I (N <sub>2</sub> )	0.4	14.3	35.9	65.0
Total (mol %)	100	100	100	100
Max H <sub>2</sub> yield (wt% of SG), Eq. 4	48.7	35.9	26.5	11.5
H <sub>2</sub> purity (Eq. (5)) at max H <sub>2</sub> yield (%) C-SR (Eq. (4))	79.1	77.2	72.2	58.5
H <sub>2</sub> purity (Eq. (5)) at max H <sub>2</sub> yield (%) SE-SR (Eq. (4))	99.9	96.0	88.7	69.0

used when there is a second step in the cyclic process, i.e., (regeneration of  $\text{CO}_2$  sorbent) while 'H' is enthalpy of formation of relevant species at the indicated temperature. It is worth noting that the enthalpy of a typical commercial steam reforming catalyst i.e. 18 wt% NiO on  $\alpha\text{-Al}_2\text{O}_3$  support was included in the energy balance, representing a packed bed reactor operation as opposed to a fluidized bed operation in the previous studies of Adiya et al. [32].

## Results and discussion

### Effect of varying composition in feedstock on SE-SR process outputs

$\text{H}_2$  yield,  $\text{H}_2$  purity and selectivity to calcium carbonate product  $\text{H}_2$  yield and purity plots over temperature range of 500–1200 K, atmospheric pressure and S:C ratio of 3 are displayed in Figs. 2 and 3(a) for the different shale gas compositions using  $\text{CaO}_{(s)}$  sorbent.  $\text{H}_2$  yield and purity was not only dependent on temperature and S:C ratio (to be discussed later) but also on the content of hydrocarbons in the gases (i.e.  $\text{SG } 1 > \text{SG } 2 > \text{SG } 3 > \text{SG } 4$ ) as well. The figures show that gases with low hydrocarbons composition had the lowest  $\text{H}_2$  yield. This was expected because of the combined effects of decreasing numerator (less moles of  $\text{H}_2$  produced from lower C and H content) and increasing denominator (increasing molar mass of fuel due to heavier inert  $\text{CO}_2$  and  $\text{N}_2$  content) in Eq. (4), as SG mixtures varied from SG1 to SG4. To further illustrate the effect of gas composition on  $\text{H}_2$  yield and purity a common case of S:C 3 with  $\text{CaO}_{(s)}$  sorbent can be used. The highest equilibrium  $\text{H}_2$  yield for SG1 was 45.5 wt% of fuel at 880 K, i.e. 93% of the maximum corresponding to complete reactions, as per Eq. (4) (Table 1). This became 34.0 wt% of fuel at 890 K for SG2 (or 95% of max.), 25.0 wt% of fuel at 880 K for SG3 (95% of max.), and 11.0 wt% of fuel at 860 K for SG4 (96% of max.). Highest equilibrium  $\text{H}_2$  yields for SG2–SG4 represented 25%, 45%, and 76% decreases compared to SG1, i.e. the same relative decreases can be calculated between the maximum  $\text{H}_2$  yield according to Eq. (4) for SG1 and the rest of the shale gases (SG2–

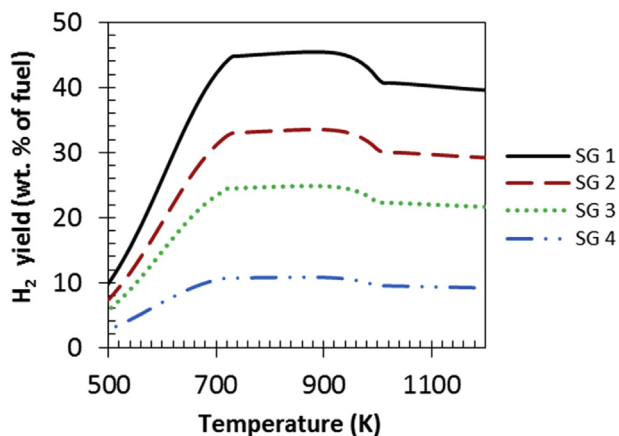


**Fig. 2 – Equilibrium  $\text{H}_2$  yield vs temperature at 1 bar, Ca:C 1 and S:C 3 for SG1–4 using  $\text{CaO}_{(s)}$  sorbent. Maximum  $\text{H}_2$  yield by complete reaction to  $\text{CaCO}_{3(s)}$  given in Table 1.**

SG4) using values shown in Table 1. This is because carbon selectivity to  $\text{CaCO}_{3(s)}$  was in excess of 90% for all the shale gases as can be seen in Fig. 3. Highest  $\text{H}_2$  purity at equilibrium was found between 720 K and 950 K followed the trend of decreasing from close to 100% for SG1, to 66% for SG4, in agreement with values calculated in Table 1, corroborating equilibrium conditions close to complete reaction to  $\text{H}_2$  and  $\text{CaCO}_{3(s)}$ . As selectivity to  $\text{CaCO}_{3(s)}$  dropped for temperatures above 950 K, the  $\text{H}_2$  purity could be seen to revert to below those given in Table 1 for C-SR values (75% vs. 79% for SG1, 50% vs. 58% for SG4), as the  $\text{CO}$  co-product from reverse water gas shift prevented the maximum purity to be reached at these higher temperatures.

One of the most significant uses of Ca sorbent in a reforming process, if not the best, is the fact that it effectively captures  $\text{CO}_2$  as depicted in Fig. 3(b). This process (carbonation reaction) is the backbone of all the benefits observed in the process from substantial increase in  $\text{H}_2$  yield and purity to significant energy savings brought about by the SE-SR process. Examples and a discussion of such energy savings can be found for SG1 in our previous publication S G Adiya et al. [32]. In Ref. [32], we show the equilibrium moles of  $\text{CaCO}_{3(s)}$  decrease gradually reaching zero with increase in temperature from approximately 960 or 990 K depending on S:C ratio for the SG considered. This was expected because of the high reaction temperature in favour of the strong endothermic decomposition of  $\text{CaCO}_{3(s)}$  [29,32,72,73]. Formation of  $\text{CaCO}_{3(s)}$  above 1000 K is not possible owing to its decomposition. In the absence of steam in the system and stoichiometric S:C ratio i.e. S:C 1, the generation of  $\text{CO}_2$  is limited by steam available for steam reforming, thus, the production of  $\text{CaCO}_{3(s)}$  is significantly low or not possible. Previous studies on SE-SR process such as Silva et al. [23], Chen et al. [24] and Dupont et al. [26] were in good agreement with the results of present studies with regards to  $\text{H}_2$  yield and purity and efficiency of  $\text{CO}_2$  capture.

### Magnitude of sorption enhancement effects due to hydrocarbon content in feed gas

SG1–4 contain varying ratios of  $\text{C}_2\text{H}_6$  and  $\text{C}_3\text{H}_8$  species with respect to  $\text{CH}_4$ . In this section we explore whether sorption enhancement effects on  $\text{H}_2$  yield and purity at medium high temperatures are affected by the nature of the hydrocarbon gases present in the shale gas. Fig. 4(a–b), which correspond to feedstocks composed in turn of 99.5 vol% of either  $\text{CH}_4$ ,  $\text{C}_2\text{H}_6$  or  $\text{C}_3\text{H}_8$ , (with 0.1 vol%  $\text{CO}_2$  and 0.4 vol% of  $\text{N}_2$ , like SG1), shows the profile of sorption enhancement in  $\text{H}_2$  yield (Eq. (6)) is not affected by the nature of the alkane gases present in the feedstock. The sorption enhancement effect in  $\text{H}_2$  purity (Eq. (7)) is seen to be minimally affected by the nature of the alkanes in the feedstock.

Similarly, sorption enhancement has a beneficial effect on the undesirable  $\text{CH}_4$  yield. Fig. 4(c) plots the decrease in %  $\text{CH}_4$  yield introduced by the presence of  $\text{CaO}$  sorbent in ratio Ca:C = 1 compared to that of the C-SR (Eq. (8)). It can be seen that, again, the % drop in  $\text{CH}_4$  yield is not affected by the nature of the alkane present in the feedstock. Thus it is expected that varying the ratio of  $\text{C}_2\text{H}_6$  and  $\text{C}_3\text{H}_8$  to  $\text{CH}_4$  will not affect the extent of the sorption enhancement effects for a given set of Ca:C ratio, S:C and temperature. The maximum combined

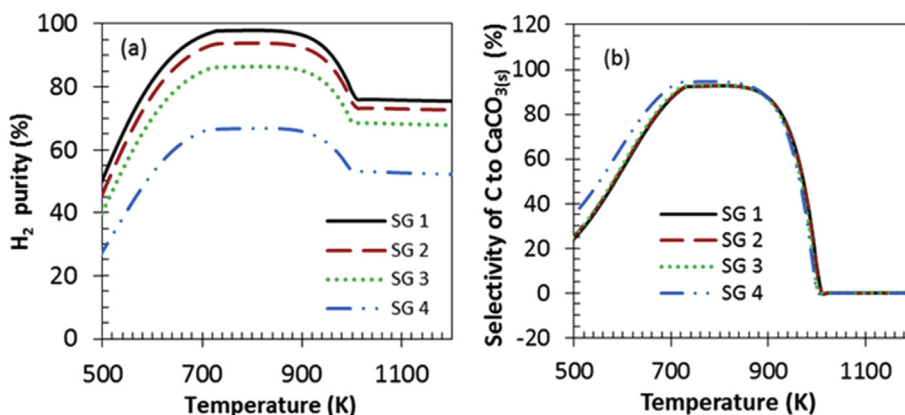


Fig. 3 – (a) H<sub>2</sub> purity vs temperature at 1 bar, Ca:C 1 and S:C 3 for shale gases 1–4, using CaO<sub>(s)</sub> sorbent (b) selectivity of carbon to CaCO<sub>3(s)</sub> vs temperature at 1 bar, Ca:C 1 and S:C 3 for shale gases 1–4, using CaO<sub>(s)</sub> sorbent. Maximum H<sub>2</sub> purity by complete reaction to CaCO<sub>3(s)</sub> given in Table 1.

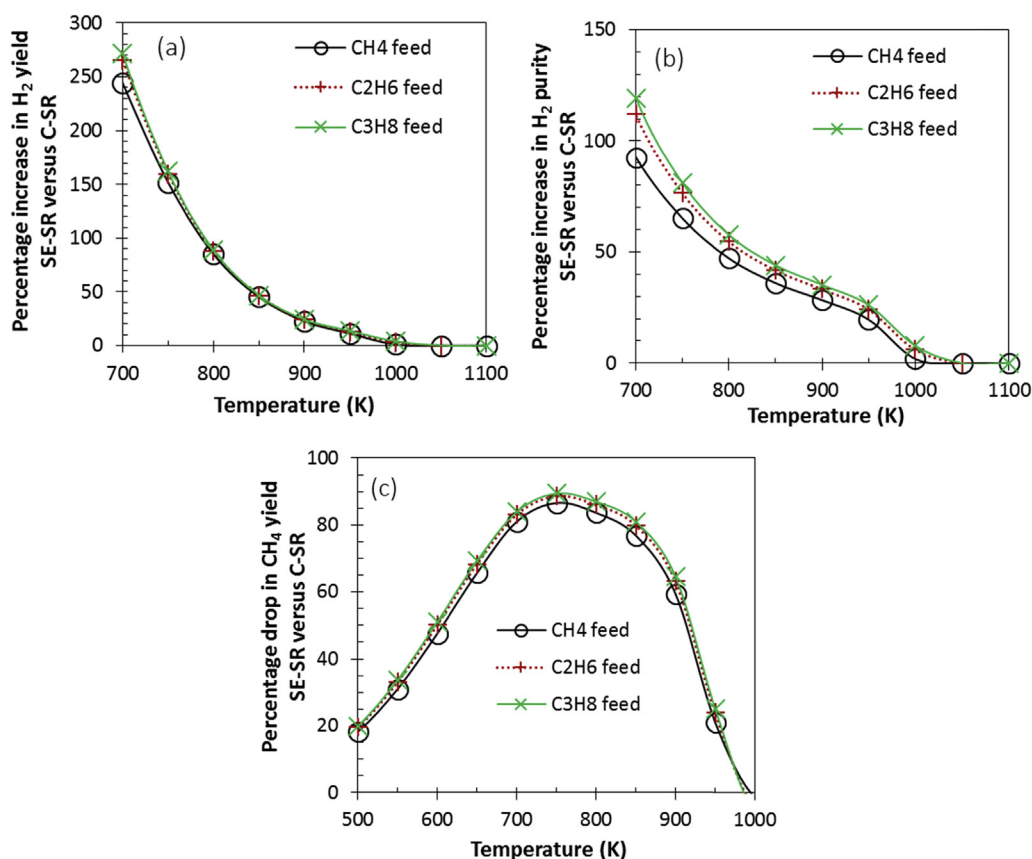


Fig. 4 – Enhancement effects at 1 bar, S:C 3 and Ca:C 1 compared to C-SR when using feedstocks of single alkane content (CH<sub>4</sub>/C<sub>2</sub>H<sub>6</sub>/C<sub>3</sub>H<sub>8</sub>) at 99.5 vol%, with 0.1 vol% CO<sub>2</sub> and 0.4 vol% N<sub>2</sub> (same inerts as in SG1). (a) % increase in H<sub>2</sub> yield (b) % increase in H<sub>2</sub> purity, (c) % drop in CH<sub>4</sub> yield.

enhancement effects by introducing the CaO sorbent in the system with Ca:C of 1 in the conditions tested are observed at 750 K, which sees the CH<sub>4</sub> yield decrease by 85–90%, concurrent with 150–160% increase in H<sub>2</sub> yield and 65–81% increase in H<sub>2</sub> purity.

*Magnitude of sorption enhancement effects due to N<sub>2</sub> and CO<sub>2</sub> content in the feed gas*

Another characteristic of the shale gases and conventional natural gases is their varying content in non-hydrocarbon gases, represented by the CO<sub>2</sub> and N<sub>2</sub>. CO<sub>2</sub> and N<sub>2</sub> content in

the feed gas may not perform the same role in the predicted equilibrium sorption enhancement effects.  $N_2$  has little participation in the main reactions, except for the little ammonia that may be predicted, its presence changes the partial pressures of the other gas species in the equilibrium system. In contrast  $CO_2$  is the product of steam reforming, water gas shift and calcium carbonate decomposition, its presence in the feed would affect not only the partial pressures of other gases but would also shift the equilibrium of these reactions.

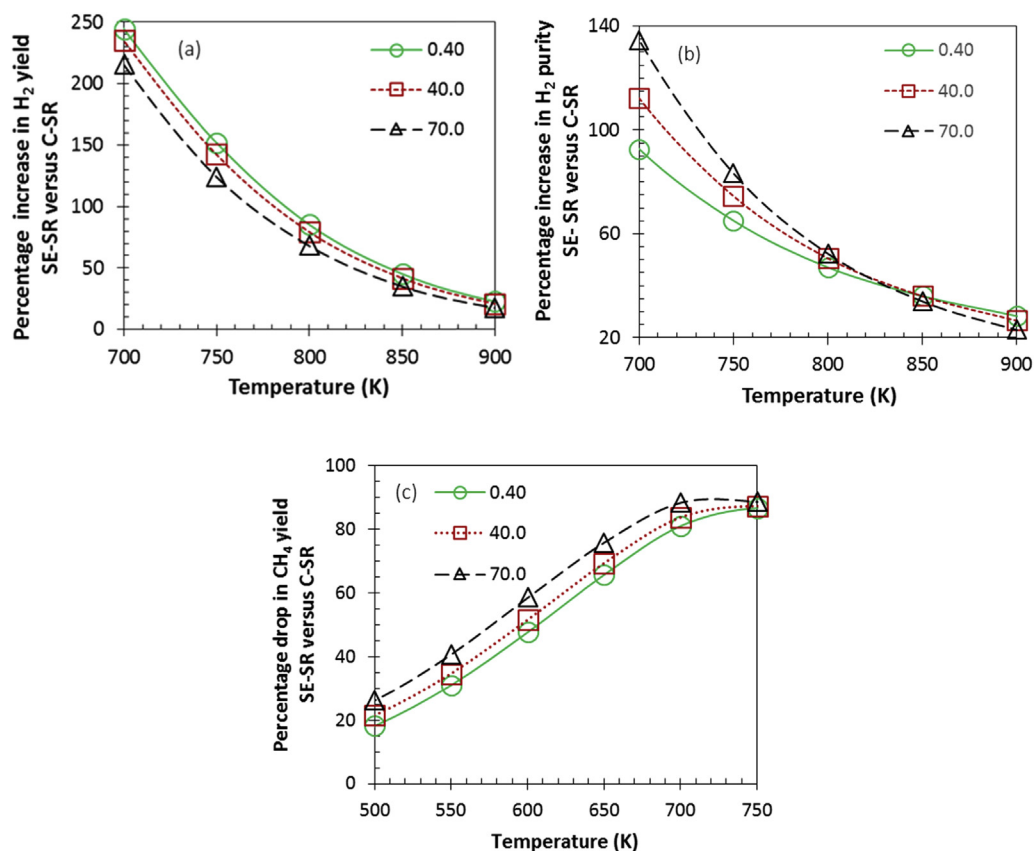
*Sorption enhancements variation with  $N_2$  content.* Fig. 5(a and b) plots the percent relative increases brought about by CaO in the steam reforming process (SE-SR at Ca:C of 1) to both  $H_2$  yield and  $H_2$  purity compared to the sorbent free system (C-SR) for varying temperatures and S:C. The feedstock chosen for the study was a composition of SG consisting of just  $CH_4$ ,  $CO_2$  (0.1 vol%, like SG1) and  $N_2$ , where  $N_2$  was varied between 0.4 vol% and 70 vol%, with increments of 10 vol%. For the purpose of clarity, Fig. 5 only shows the results for  $N_2$  in the feed gas of 0.4, 40 and 70 vol %.

Fig. 5(c) shows the percent relative drop in  $CH_4$  yield caused by a Ca:C of 1 in the steam reforming process (SE-SR) compared to the Ca-free process (C-SR). It can be seen that increasing the inert gas  $N_2$  in the feed has small but non negligible effects on the enhancement effects as measured by increases in  $H_2$  yield and purity as well as drop in  $CH_4$  yield (i.e.,

increase in  $CH_4$  conversion). For a given reforming temperature, as  $N_2$  vol% increases in the feed, the enhancement on  $H_2$  yield decreases, that on  $H_2$  purity increases, while the inhibition of  $CH_4$  yield increases. For the whole range of  $N_2$  vol%, the inhibition of  $CH_4$  yield peaked at 750 K, beyond which the differences in inhibition of  $CH_4$  yield disappeared, and all inhibition effect was negligible at 1000 K. Given that sorption enhanced steam reforming at 1 atm and S:C of 3 would be conducted at temperatures above 700 K and below 900 K to maximise  $H_2$  yield and purity (Figs. 2 and 3a), then highest enhancement effects would be achieved for feed gas with little  $N_2$  dilution.

*Sorption enhancements variation with  $CO_2$  content in the feed.* The range of  $CO_2$  content in the feed gas investigated here is 0.1–40 vol%, as  $CO_2$  content is unlikely to exceed 40 vol% (typical of biogas composition). Enhancements effects were considered for feed gases with only  $CH_4$  as the hydrocarbon content, with a Ca:C of 1 which included the carbon from the  $CO_2$  in the feed, and a  $N_2$  vol% of 0.4 (as in SG1). Fig. 6(a-c) shows the increases in  $H_2$  yield and  $H_2$  purity and the drop in  $CH_4$  yield of SE-SR vs. the C-SR.

For the range of  $CO_2$  content investigated (0.1–40 vol%), increases in  $H_2$  yield between SE-SR and C-SR were more significant for the larger  $CO_2$  content and for lower temperatures. The difference in enhancement between the different  $CO_2$  contents dropped steadily with increasing temperature. A



**Fig. 5 – Enhancement effects at 1 bar, S:C 3 and Ca:C 1 compared to C-SR when using feedstocks of single alkane content  $CH_4$ , with 0.1 vol%  $CO_2$  and varying  $N_2$  content between 0.4 and 70 vol% (a) % increase in  $H_2$  yield (b) % increase in  $H_2$  purity, (c) % drop in  $CH_4$  yield.**

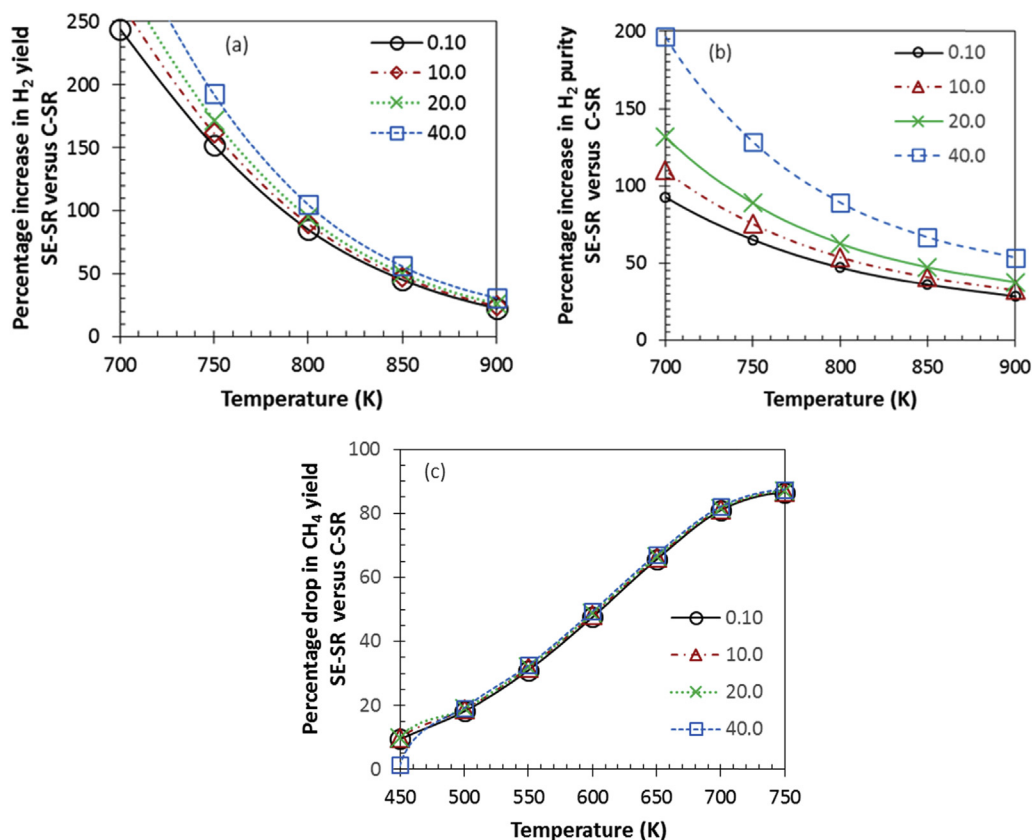


**Fig. 6** – Enhancement effects at 1 bar, S:C 3 and Ca:C 1 compared to C-SR when using feedstocks of single alkane content CH<sub>4</sub>, with 0.4 vol% N<sub>2</sub> and varying CO<sub>2</sub> content between 0.1 and 40 vol% (a) % increase in H<sub>2</sub> yield (b) % increase in H<sub>2</sub> purity, (c) % drop in CH<sub>4</sub> yield.

similar effect was found for H<sub>2</sub> purity. This can be explained by the presence of the CO<sub>2</sub> sorbent in Ca to feed Carbon molar ratio of 1 acting in two ways, as capture of the inert feed CO<sub>2</sub> and as equilibrium shift agent by removing a gas reaction product of steam reforming and water gas shift, unlike the inert N<sub>2</sub>. In contrast, the drop in CH<sub>4</sub> yield in the temperature region favourable to methanation was found to be insensitive to CO<sub>2</sub> content, and peaked at 750 K.

Performing tests at higher vol% of CO<sub>2</sub> than 40 vol% yielded contrasting results with those obtained below 40 vol% and were attributed to a CO<sub>2</sub>: hydrocarbon C ratio larger than 1, resulting in significant solid carbon product predicted for the C-SR equilibrium and non-monotonic enhancement effects for SE-SR compared to C-SR (not shown).

#### Enhancement effects of SE-SR vs. C-SR for SG1-4

Differences in SG1, SG2, SG3 and SG4's compositions, which represent real shale gases, are characterised by their varying C1+ alkane content, ie. 4.5–20.1 vol% of (C<sub>2</sub>H<sub>6</sub> + C<sub>3</sub>H<sub>8</sub>), almost constant CO<sub>2</sub> content (0–3%), and significantly changing N<sub>2</sub> content (0.4–65.0 vol%), with several species compositions altering simultaneously from one SG to the next. It was determined previously that for a given reforming temperature and S:C ratio, percent increases in H<sub>2</sub> yield and percent drops in CH<sub>4</sub> yield (SE-SR vs. C-SR) were not sensitive individually to either presence of C1+ content (CH<sub>4</sub>/C<sub>2</sub>H<sub>6</sub>/C<sub>3</sub>H<sub>8</sub>) in the feed, nor to CO<sub>2</sub> content in the 0.1–10.0 vol% range, but were

slightly affected by varying N<sub>2</sub> content in the 0.4–70.0 vol% range. This explains that the percent increases in H<sub>2</sub> yield and purity, and percent drops in CH<sub>4</sub> yield when considering in turn SG1-4, exhibited also a small quasi linear dependence on the N<sub>2</sub> content in the shale gas, but not on their other compounds. This is illustrated in Fig. 7 below.

#### Effect of temperature on SE-SR process output

Maximum water and minimum CO<sub>2</sub> yield in the equilibrium products was seen in the low temperature zone in agreement with methanation reactions. The methane conversion was

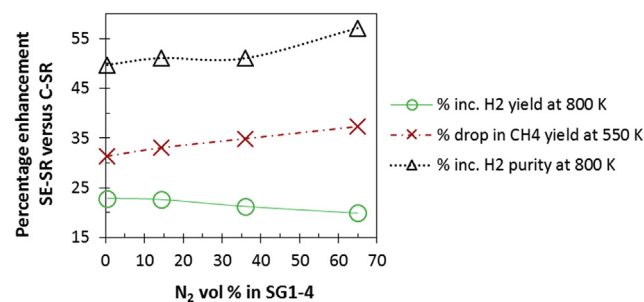


**Fig. 7** – Magnitude of enhancement effects between SE-SR and C-SR as function of N<sub>2</sub> content in the shale gases SG1-4, represented by percent increases in H<sub>2</sub> yield and purity at 800 K and % drop in CH<sub>4</sub> yield at 550 K.

particularly negative (output higher than the input) in the low temperature range (298–540 K). As temperature rose the yield of methane dropped gradually, and CO<sub>2</sub> dominated. Nearly complete conversion of fuel (shale gas) was observed for all the temperatures investigated. Both shale gases required temperature in the range of 900–1000 K to undergo thermal decomposition and begin converting significantly to H<sub>2</sub> at S:C 0. For S:C of 1, 2, and 3, H<sub>2</sub> yield and purity increased steeply as temperature increased (Figure not shown). This was caused by shift from the strongly exothermic methanation reaction favoured at low temperature to endothermic steam methane reforming favoured at high temperatures. As soon as a certain point limit is reached, at about 700 K approximately, H<sub>2</sub> yield and purity stabilised and then declined at a point, where a gentle dwindling in H<sub>2</sub> yield and purity is seen, independent of the S:C ratio. This is caused by the reverse water gas shift reaction which tends to dominate at higher temperatures. The main equilibrium products from the gas-water system at S:C ratio of 1, 2, and 3 are; CH<sub>4</sub>, CO, CO<sub>2</sub>, and H<sub>2</sub>, with the later (H<sub>2</sub>) dominating in the medium/high temperature range. Steam reforming took place significantly, dominating methanation reaction at roughly 700 K (427 °C), as described by a sharp increase in H<sub>2</sub> yield in Fig. 2. The condition of S:C 3, Ca:C 1 and 1 bar indicated maximum equilibrium H<sub>2</sub> yield and purity. It is interesting to note that the optimum temperature for SE-SR is in the range of 800–900 K approximately based on the maximum equilibrium output (see [supplementary data](#)). The temperature range also corresponds to the range of maximum CO<sub>2</sub> sorption to CaCO<sub>3(s)</sub> as depicted in Fig. 3(b).

#### *Effect of steam to carbon ratio on process outputs*

Nearly complete water conversion (e.g. 99.9% at 500 K maximum for shale gas '2') was seen at S:C 1 with CaO<sub>(s)</sub> sorbent in the system, no doubt this is because stoichiometric amount of water (reactant) was provided to the system. At S:C ratio of 2 and 3 incomplete water conversion was seen because water was provided in excess to the system (see [supplementary data for maximum conversion](#)). It was found that the effect of S:C ratio for the four SG was also dependent on the gas composition. The term 'S:C ratio' defined here as the total moles of water inputted divided by the total moles of carbon species in the feed. Consequently, the higher the moles of carbon species in the feedstock, the higher the moles of water to be used as reactant. Thus, contributing to the high H<sub>2</sub> yield, decreasing with decreasing number of carbon species in the feedstock which corresponds to decreasing concentration of water in the system. Although the maximum steam conversion (at the varied S:C ratio) was in the same range for all the varied gases, for example at S:C ratio of 3, steam conversion was in the range of 63–64% for all the four shale gases, with almost no or negligible difference.

Generally speaking, steam variation (a reactant in both reforming and the water gas shift reaction process) can significantly affect the equilibrium of both reactions. S:C ratio was varied in the range of 0–3, higher values were not considered as previous study by S G Adiya et al. [32] and Antzara et al. [74] have shown that S:C ratios higher than 4 do not have any significant further effect on H<sub>2</sub> yield and purity. The variation of S:C ratio in SE-SR process is in agreement with Le Chatelier's principle in all the four varied gas

composition, whereby an increase in the water concentration in the system favours the equilibrium of the H<sub>2</sub> producing reactions towards conversion of the excess water into H<sub>2</sub>, thus triggering higher H<sub>2</sub> yield and purity.

#### *Effect of inert bed materials, hydrocarbon fractions, inert N<sub>2</sub> and CO<sub>2</sub> and on enthalpy balance*

##### *Effect of inert bed materials on energy balance*

Reduced energy demand was caused by the carbonation reaction in the SE-SR process even though a complete regeneration of the CaCO<sub>3(s)</sub> back to CaO<sub>(s)</sub> via a decarbonation step was conducted at 1170 K in the presence of a typical commercial steam reforming catalyst (18 wt% NiO on  $\alpha$ -Al<sub>2</sub>O<sub>3</sub> support). The equilibrium materials balances were not affected by the presence of non-reacting solid materials in the reactor bed (catalyst and its support, and the fresh and degraded sorbent). In other words, H<sub>2</sub> yield and purity are the same with non-reacting solid materials compared to without, as they do not have any influence on them. However, non-reacting bed materials significantly affect the energy of operating the system. This is because they would require heating or cooling as required during the operation. This is further demonstrated in Fig. 8(a) depicting the  $\Delta H$  ratio of shale gas 3 (used for demonstration) with degraded sorbent been higher than the system without degraded sorbent at exactly same operating condition. The effect of degraded sorbent in the bed was represented by introducing in the reactants mix the equivalent of 90 wt% of the total molar calcium in the feed as inert CaO. The Ca:C ratio of 1 quoted in the figures refers to the active CaO. The  $\Delta H$  ratios of the system with degraded sorbent were seen to increase compared to the system with active sorbent only by 0.118 at 880 K (region of maximum H<sub>2</sub> yield and purity), with a narrowing gap as the reforming temperature approached the regeneration temperature of 1170 K. This no doubt can be attributed to the enthalpy cost of heating the degraded sorbent as shown in Fig. 8(c), increasing the total enthalpy of the entire process as depicted by Fig. 8(b).

##### *Effect of hydrocarbon fractions on enthalpy balance*

The cost of heating up the gas was relatively insignificant compared to those of raising steam from liquid water feed. The total energy cost of the process was dominated by water enthalpy change accounting for over 70% approximately of the total energy required to heat the cold reactants. Using shale gas termed '1' for example at 880 K (region of maximum H<sub>2</sub> yield and purity) 88% of the total energy required to heat the cold reactants was dominated by water. However, this decreased to 86%, 84% and 77% for shale gas termed 2, 3 and 4 respectively at same conditions. This was expected since the concentration of water in each of the system was based on number of carbon concentration explained earlier. This compromise the choice of gas feedstock with high hydrocarbon content; between high cost of raising excess steam (cause by the use of high S:C ratio) balance by higher H<sub>2</sub> yield and purity (cause by the high hydrocarbon content in the feedstock). Fig. 9 further help in analysing the energetic cost of operating with each of the SGs. Although not particularly significant because they depend on the molar inputs chosen for the system, what matters is the relative positions of each

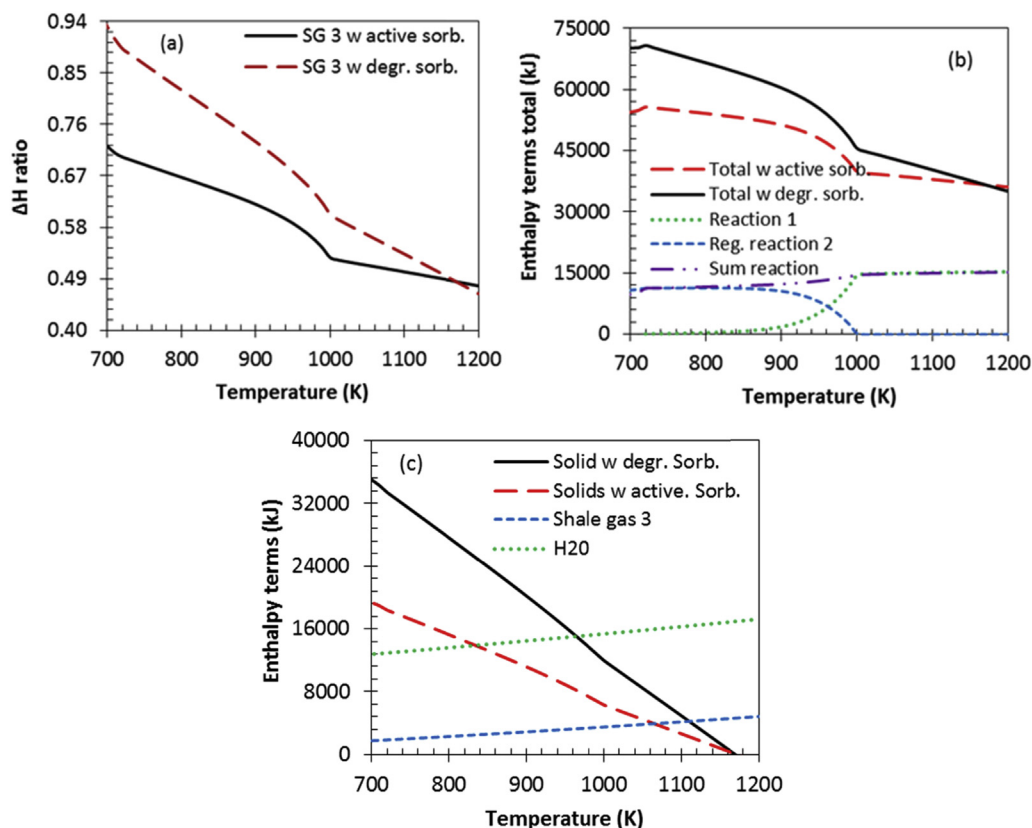


**Fig. 8** – Enthalpy terms for SG3, catalyst 18 wt% NiO/Al<sub>2</sub>O<sub>3</sub>, active Ca:C 1, S:C 3 (a)  $\Delta H$  ratio vs temperature, (b) and (c) enthalpy terms vs temperature: process 2 at 1170 K, “active Sorb.”: 100% CaO, “degr. Sorb.”: 10% active CaO and 90% inert CaO.

enthalpy term profiles in the figure. The figure clearly depicts that it is more energetically costly to operate with shale gas termed 1 compared 2, 3 and 4. This energetic cost is found to be dominated by enthalpy of raising steam which is dependent on the carbon specie concentration in each of the gas.

No significant difference was found between the  $\Delta H$  ratio and total enthalpy terms in kJ/mol of H<sub>2</sub> produced of SG1-3. However, significant difference was observed between SG1 and SG4 as shown in Fig. 10 caused by the significant

concentration of N<sub>2</sub> in SG4 costing 12.00% at 880 K of the total energy required in heating the cold reactants as opposed to 0.03% for SG1, 1.25% and 4.00% for SG2 and SG3 respectively at same operating condition. The effect of N<sub>2</sub> and CO<sub>2</sub> gas fractions on steam reforming process will be discussed in more detail in the next section.

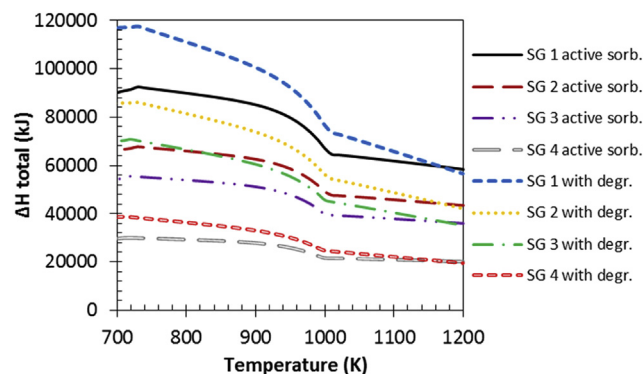


**Fig. 9** –  $\Delta H$  total vs. temperature for 18 wt% NiO/Al<sub>2</sub>O<sub>3</sub> catalyst, active Ca:C 1, S:C 3 and SG1-4: process 2 at 1170 K, “active Sorb.”: 100% CaO, “degr. Sorb.”: 10% active CaO and 90% inert CaO.

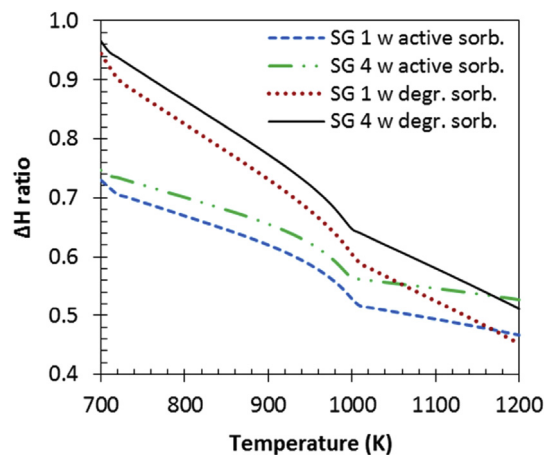


**Fig. 10** –  $\Delta H$  ratio vs temperature comparing SG1-4: for 18 wt% NiO/Al<sub>2</sub>O<sub>3</sub> catalyst, active Ca:C 1, S:C 3 and process 2 at 1170 K: “active sorbent”: 100% CaO, “degraded sorbent”: 10% active CaO and 90% inert CaO.

*Effect of N<sub>2</sub> and CO<sub>2</sub> content in the feed gas on enthalpy balance*  
Although most gases contain inert species with varied concentrations according to their source (from 1 to over 40%) [75] as reflected in the N<sub>2</sub> contents listed in Table 1, a gas with high hydrocarbon content and reasonable inert composition is more suitable for steam reforming from almost all perspective especially the economic part. A gas with significantly high inerts contents, as reflected by N<sub>2</sub> concentration in SG3 and SG4 particularly affects the cost of reforming plants significantly in a very negative way. This is because the energy of heating up the inert gas flow adds to the total energy of the whole process, thus increasing the cost of operating the plant. Moreover, inert gases do not directly generate H<sub>2</sub>, hence, their presence in the system has relatively no significance to H<sub>2</sub> generation. Nonetheless, a positive effect of inert gas content in the shale gas is that the partial pressure of the N<sub>2</sub> reduces that of the reactants (e.g CH<sub>4</sub> and steam) in the system, thus favouring the equilibrium of the steam reforming process in accordance with Le Chatelier's principle and as proved by several laboratory scale studies [21].

The effect of CO<sub>2</sub> in the shale gas feedstock, has, by comparison a more negative effect on the SR due to CO<sub>2</sub> being one of the desirable products of the shale gas conversion and the equilibrium shift towards methanation and reverse water gas shift at medium temperatures. However, gases with significant amount of CO<sub>2</sub> can generate H<sub>2</sub> through dry reforming of CH<sub>4</sub> at higher temperatures (R5) [76,77], but studies on the rate of the reaction while occurring simultaneously with steam reforming are limited/not available. For the SE-SR process, significant concentration or flow of CO<sub>2</sub> can lead to fast saturation of the sorbent, which in turn will increase the cost of operation either by frequent regeneration of the sorbent or require over-sizing of the sorbent bed. The increased frequency of regeneration may also result in faster loss of sorbent capacity owing to deactivation over repeated use. According to an experiment represented by Laosiripojana et al. [75], both CO<sub>2</sub> and H<sub>2</sub>S inhibit methane steam reforming rate over both catalysts (Ni/CeO<sub>2</sub> and Ni/Al<sub>2</sub>O<sub>3</sub>) investigated and subsequently caused a decreased on H<sub>2</sub> production yield.

## Conclusion and final remarks

A detailed thermodynamic equilibrium analysis of four varied shale gas composition (as represented by content in higher hydrocarbon, inert N<sub>2</sub> and CO<sub>2</sub> gas in the various gases, with methane always being the main hydrocarbon component) in the presence of CaO sorbent for H<sub>2</sub> production has been conducted. The influence of hydrocarbon fractions, temperature, S:C ratio, inert N<sub>2</sub>, CO<sub>2</sub> gas and inert bed materials on equilibrium yield and enthalpy balance has been investigated. The analysis yielded the following fundamental insights and recommendations:

- H<sub>2</sub> yield and purity was not only dependent on temperature and S:C ratio but also on the content of hydrocarbons in the gases. H<sub>2</sub> yield and purity decrease in succession of the hydrocarbon content (i.e. SG 1 > SG 2 > SG 3 > SG 4). Up to 25%, 45% and 76% decrease in maximum H<sub>2</sub> yield was seen

in SG2-4 respectively compared to SG1 with the highest hydrocarbon content.

- The magnitude of enhancement effects brought on by sorption enhanced steam reforming compared to conventional steam reforming at given temperature and steam to carbon ratio are not dependent on the alkane mix, nor the CO<sub>2</sub> content in the feed (0.1–10 vol %), but slightly dependent on the nitrogen content in the feed (0.4–70 vol%), with larger H<sub>2</sub> purity enhancement but lower H<sub>2</sub> yield enhancement for larger N<sub>2</sub> content, inhibition of methanation is also larger for larger N<sub>2</sub> content at temperatures below 750 K.
- Gases with high hydrocarbon composition have also higher energetic cost of operation than gases with lower hydrocarbon content.
- The conditions of S:C 3, 1 bar, and temperature range of 800–900 K are optimal conditions of SE-SR process.
- SE-SR could have considerable advantages for H<sub>2</sub> production because of the substantial increase in H<sub>2</sub> yield and purity, as well as significant drop in temperature of the maximum H<sub>2</sub> yield with effective capture of CO<sub>2</sub> under well-chosen operational conditions.
- Near full sorption enhancement (over 90% efficiency of CO<sub>2</sub> capture) was seen in the temperature range of about 880–900 K, this will reduce, if not eliminate, the need for further purification steps required in C-SR as well as minimise the cost of operating the system, depending on the purity requirement and end use of the H<sub>2</sub> produced.
- The opportunity of operating the system at low temperature (due to the presence of Ca sorbent) could in turn decrease the need to operate at high pressure, thus, favouring the H<sub>2</sub> producing reactions.
- The presence of degraded CO<sub>2</sub> sorbent in the reactor bed introduces a heating burden associated with heating the material from reforming temperature to sorbent regeneration temperature.

## Acknowledgement

The Petroleum Technology Development Fund (Nigeria) is gratefully acknowledged for the scholarship of Zainab Ibrahim S. G. Adiya, and we also thank the UKCCSRC EPSRC consortium (EP/K000446/1) for call 2 grant 'Novel Materials and Reforming Process Route for the Production of Ready-Separated CO<sub>2</sub>/N<sub>2</sub>/H<sub>2</sub> from Natural Gas Feedstocks'.

Data used to generate tables and graphs in this publication can be found at <http://dx.doi.org/10.5518/217>.

## Appendix A. Supplementary data

Supplementary data related to this article can be found at <http://dx.doi.org/10.1016/j.ijhydene.2017.06.169>.

## REFERENCES

- [1] Ryden M, Ramos P. H<sub>2</sub> production with CO<sub>2</sub> capture by sorption enhanced chemical-looping reforming using NiO as

- oxygen carrier and CaO as CO<sub>2</sub> sorbent. *Fuel Process Technol* 2012;96:27–36.
- [2] Paltsev S, Jacoby HD, Reilly JM, Ejaz QJ, Morris J, O'Sullivan F, et al. The future of U.S. natural gas production, use, and trade. *Energy Policy* 2011;39:5309–21.
  - [3] Anderson DM, Kottke PA, Fedorov AG. Thermodynamic analysis of hydrogen production via sorption-enhanced steam methane reforming in a new class of variable volume batch-membrane reactor. *Int J Hydrogen Energy* 2014;39:17985–97.
  - [4] Nicholls T, Gorst I, Lewis L, Ruddy M. Everything you wanted to know about gas... But were afraid to ask. London: Silverstone communications Ltd (Energy Future); 2012.
  - [5] Banking on U.S. Shale gas boom. Asia petrochemical firms switch to LPG. 2014. <http://www.reuters.com/article/2014/08/21/us-asia-lpg-idUSKBN0GL2AD20140821> [Accessed 29.August.14].
  - [6] Steam Reforming 50 years of developments and the challenges for the next 50 years. Uhde GmbH; 2005. [http://www.uhde-ftp.de/cgi-bin/byteserver.pl/archive/upload/uhde\\_publications\\_pdf\\_en\\_53.00.pdf](http://www.uhde-ftp.de/cgi-bin/byteserver.pl/archive/upload/uhde_publications_pdf_en_53.00.pdf) [Accessed 29.August.14].
  - [7] Annual energy Outlook 2017 with projections to 2050. Administration USEI. 2017. <https://www.eia.gov/outlooks/aeo/pdf/0383%282017%29.pdf> [Accessed 3.March.17].
  - [8] The effects of shale gas production on natural gas prices. PPI Energy and Chemicals Team. U.S. Bureau of Labor Statistics. 2013. [https://www.bls.gov/opub/btn/volume-2/the-effects-of-shale-gas-production-on-natural-gas-prices.htm?view\\_full](https://www.bls.gov/opub/btn/volume-2/the-effects-of-shale-gas-production-on-natural-gas-prices.htm?view_full) [Accessed 21.February.17].
  - [9] Shale gas production in the United States from 1999 to 2015 (in trillion cubic feet). The Statistics Portal:Statista. 2015. <https://www.statista.com/statistics/183740/shale-gas-production-in-the-united-states-since-1999/> [Accessed 21.February.17].
  - [10] Ramachandran R, Menon RK. An overview of industrial uses of hydrogen. *Int J Hydrogen Energy* 1998;23:593–8.
  - [11] Hydrogen (H<sub>2</sub>) properties, uses, applications hydrogen gas and liquid hydrogen. Universal Industrial Gases; 2008. <http://www.ugi.com/hydrogen.html> [Accessed 21.February.17].
  - [12] Hamad TA, Agil AA, Hamad YM, Bapat S, Thomas M, Martin KB, et al. Hydrogen recovery, cleaning, compression, storage, dispensing, distribution system and End-Uses on the university campus from combined heat, hydrogen and power system. *Int J Hydrogen Energy* 2014;3(9):647–53.
  - [13] Cecere D, Giacomazzi E, Ingenito A. A review on hydrogen industrial aerospace applications. *Int J Hydrogen Energy* 2014;39:1–17.
  - [14] Chirona F-X, Patiencea GS, Riffartb S. Hydrogen production through chemical looping using NiO/NiAl<sub>2</sub>O<sub>4</sub> as oxygen carrier. *Chem Eng Sci* 2011;66:6324–30.
  - [15] Harrison DP, Peng Z. Low-carbon monoxide hydrogen by sorption enhanced reaction. *IJCRE* 2003;1. 1542–6580.
  - [16] Optimising hydrogen production and use. UOP LLC, A Honeywell Company; 2011. <https://www.uop.com/?document=ptq-optimising-h2-production-and-use&download=1> [Accessed 1.March.17].
  - [17] World hydrogen. The Freedonia Group Inc; 2014. <https://www.freedoniagroup.com/brochure/28xx/2895smwe.pdf> [Accessed 30.November.16].
  - [18] Kumar RV, Lyon RK, Cole JA. Unmixed reforming: a novel autothermal cyclic steam reforming process. US: Springer; 2002.
  - [19] Rostrup-Nielsen JR, Sehested J, Nørskov JK. Hydrogen and synthesis gas by steam- and CO<sub>2</sub> reforming. *Adv Catal* 2000;47:65–137.
  - [20] Simpson AP, Lutz AE. Exergy analysis of hydrogen production via steam methane reforming. *Int J Hydrogen Energy* 2007;32:4811–20.
  - [21] Zhu J, Zhang D, King KD. Reforming of CH<sub>4</sub> by partial oxidation: thermodynamic and kinetic analyses. *Fuel* 2001;80:899–905.
  - [22] Budiman AW, Song S-H, Chang T-S, Shin C-H, Choi M-J. Dry reforming of methane over cobalt catalysts: a literature review of catalyst development. *Catal Surv Asia* 2012;16:183–97.
  - [23] Lima da Silva A, Müller IL. Hydrogen production by sorption enhanced steam reforming of oxygenated hydrocarbons (ethanol, glycerol, n-butanol and methanol): thermodynamic modelling. *Int J Hydrogen Energy* 2011;36:2057–75.
  - [24] Chen H, Zhang T, Dou B, Dupont V, Williams P, Ghadiri M, et al. Thermodynamic analyses of adsorption-enhanced steam reforming of glycerol for hydrogen production. *Int J Hydrogen Energy* 2009;34:7208–22.
  - [25] Dou B, Jiang B, Song Y, Zhang C, Wang C, Chen H, et al. Enhanced hydrogen production by sorption-enhanced steam reforming from glycerol with in-situ CO<sub>2</sub> removal in a fixed-bed reactor. *Fuel* 2016;166:340–6.
  - [26] Dupont V, Twigg MV, Rollinson AN, Jones JM. Thermodynamics of hydrogen production from urea by steam reforming with and without in situ carbon dioxide sorption. *Int J Hydrogen Energy* 2013;38:10260–9.
  - [27] Johnsen K, Ryu HJ, Grace JR, Lim CJ. Sorption-enhanced steam reforming of methane in a fluidized bed reactor with dolomite as CO<sub>2</sub>-acceptor. *Chem Eng Sci* 2006;61:1195–202.
  - [28] Reijers HTJ, Valster-Schiermeier SEA, Cobden PD, van den Brink RW. Hydrotalcite as CO<sub>2</sub> sorbent for sorption-enhanced steam reforming of methane. *Ind Eng Chem Res* 2006;45:2522–30.
  - [29] Wang X, Wang N, Wang L. Hydrogen production by sorption enhanced steam reforming of propane : a thermodynamic investigation. *Int J Hydrogen Energy* 2011;36:466–72.
  - [30] Iordanidis AA, Kechagiopoulos PN, Voutetakis SS, Lemonidou AA, Vasalos IA. Autothermal sorption-enhanced steam reforming of bio-oil/biogas mixture and energy generation by fuel cells: concept analysis and process simulation. *Int J Hydrogen Energy* 2006;31:1058–65.
  - [31] Yang S, Xu X, Tian W. Simulation for hydrogen production from sorption enhanced coke oven gas steam reforming based on chemical looping combustion. *J Che Ind Eng China* 2007;58:2363.
  - [32] Adiya ZI SG, Dupont V, Mahmud T. Chemical equilibrium analysis of hydrogen production from shale gas using sorption enhanced chemical looping steam reforming. *Fuel Process Technol* 2017;159:128–44.
  - [33] Ni M, Leung DY, Leung MKH. A review on reforming bio-ethanol for hydrogen production. *Int J Hydrogen Energy* 2007;32:3238–47.
  - [34] Md Zin R, Ross AB, Jones JM, Dupont V. Hydrogen from ethanol reforming with aqueous fraction of pine pyrolysis oil with and without chemical looping. *Bioresour Technol* 2015;176:257–66.
  - [35] Rosen MA. Thermodynamic investigation of hydrogen production by steam-methane reforming. *Int J Hydrogen Energy* 1991;16:207–17.
  - [36] Pasel J, Samsun RC, Tschauder A, Peters R, Stolten D. A novel reactor type for autothermal reforming of diesel fuel and kerosene. *Appl Energy* 2015;150:176–84.
  - [37] LeValley TL, Richard AR, Fan M. The progress in water gas shift and steam reforming hydrogen production technologies – a review. *Int J Hydrogen Energy* 2014;39:16983–7000.
  - [38] Adris AM, Pruden BB, Lim CJ, Grace JR. On the reported attempts to radically improve the performance of the steam methane reforming reactor. *Can J Chem Eng* 1996;74:177–86.
  - [39] Fernández JR, Abanadesa JC, Murillo R, Grasab G. Conceptual design of a hydrogen production process from

- natural gas with CO<sub>2</sub> capture using a Ca–Cu chemical loop. *Int J Greenh Gas Con* 2012;6:126–41.
- [40] Patel N, Baade B, Fong LW, Khurana V. Creating value through refinery hydrogen management. Singapore: Asian Refinery Technology Conference; 2006.
- [41] Market conditions encourage refiners to recover by-product gases. 2013. In: <http://www.ogj.com/articles/print/volume-111/issue-10/processing/market-conditions-encourage-refiners-to-recover.html> [Accessed 6.June.17].
- [42] Yildirim Ö, Kiss AA, Hüser N, Leßmann K, Kenig EY. Reactive absorption in chemical process industry: a review on current activities. *Chem Eng J* 2012;213:371–91.
- [43] Adhikari S, Fernando S. Hydrogen membrane separation techniques. *Ind Eng Chem Res* 2006;45:875–81.
- [44] Hafizi A, Rahimpour MR, Hassanajili S. High purity hydrogen production via sorption enhanced chemical looping reforming: application of 22Fe<sub>2</sub>O<sub>3</sub>/MgAl<sub>2</sub>O<sub>4</sub> and 22Fe<sub>2</sub>O<sub>3</sub>/Al<sub>2</sub>O<sub>3</sub> as oxygen carriers and cerium promoted CaO as CO<sub>2</sub> sorbent. *App Energy* 2016;169:629–41.
- [45] Chaubey R, Sahu Satanand, James Olusola O, Maity Sudip. A review on development of industrial processes and emerging techniques for production of hydrogen from renewable and sustainable sources. *Renew Sust Energy Rev* 2013;23:443–62.
- [46] Ochoa-Fernandez E, Haugen G, Zhao T, Ronning M, Aartun I, Borresen B, et al. Process design simulation of H<sub>2</sub> production by sorption enhanced steam methane reforming: evaluation of potential CO<sub>2</sub> acceptors. *Green Chem* 2007;9:654–62.
- [47] Broda M, Manovic V, Imtiaz Q, Kierzkowska AM, Anthony EJ, Müller CR. High-Purity hydrogen via the sorption-enhanced steam methane reforming reaction over a synthetic CaO-based sorbent and a Ni catalyst. *Environ Sci Technol* 2013;47:6007–14.
- [48] van Selow ER, Cobden PD, Verbraeken PA, Hufton JR, van den Brink RW. Carbon capture by sorption-enhanced Water–Gas shift reaction process using hydrotalcite-based material. *Ind Eng Chem Res* 2009;48:4184–93.
- [49] Barelli L, Bidini G, Gallorini F, Servili S. Hydrogen production through sorption-enhanced steam methane reforming and membrane technology: a review. *Energy* 2008;33:554–70.
- [50] Sun P, Lim CJ, Grace JR. Cyclic CO<sub>2</sub> capture by limestone-derived sorbent during prolonged calcination/carbonation cycling. *AIChE J* 2008;54:1668–77.
- [51] Lysikov AI, Salanov AN, Okunev AG. Change of CO<sub>2</sub> carrying capacity of CaO in isothermal Recarbonation–Decomposition cycles. *Ind Eng Chem Res* 2007;46:4633–8.
- [52] Shokrollahi Yancheshmeh M, Radfarnia HR, Iliuta MC. High temperature CO<sub>2</sub> sorbents and their application for hydrogen production by sorption enhanced steam reforming process. *Chem Eng J* 2016;283:420–44.
- [53] Zhou Z, Xu P, Xie M, Cheng Z, Yuan W. Modeling of the carbonation kinetics of a synthetic CaO-based sorbent. *Chem Eng Sci* 2013;95:283–90.
- [54] Sedghkerdar MH, Mahinpey N, Sun Z, Kaliaguine S. Novel synthetic sol–gel CaO based pellets using porous mesostructured silica in cyclic CO<sub>2</sub> capture process. *Fuel* 2014;127:101–8.
- [55] Zhang X, Li Z, Peng Y, Su W, Sun X, Li J. Investigation on a novel CaO–Y<sub>2</sub>O<sub>3</sub> sorbent for efficient CO<sub>2</sub> mitigation. *Chem Eng J* 2014;243:297–304.
- [56] Yu C-T, Chen W-C. Preparation, characterization of Ca/Al carbonate pellets with TiO<sub>2</sub> binder and CO<sub>2</sub> sorption at elevated-temperature conditions. *Powder Technol* 2013;239:492–8.
- [57] Wu SF, Wang LL. Improvement of the stability of a ZrO<sub>2</sub>-modified Ni–nano-CaO sorption complex catalyst for ReSER hydrogen production. *Int J Hydrogen Energy* 2010;35:6518–24.
- [58] García-Lario AL, Grasa GS, Murillo R. Performance of a combined CaO-based sorbent and catalyst on H<sub>2</sub> production, via sorption enhanced methane steam reforming. *Chem Eng J* 2015;264:697–705.
- [59] Storset SO, Brunsvold A, Jordal K, Langorge O, Anantharaman R, Berstad D, et al. Technology survey and assessment for piloting of CO<sub>2</sub> capture technologies. SINTEF Energy Reserch Gas Technol 2013.
- [60] Pfeifer C, Prolly T, Puchnerz B, Hofbauer H. H<sub>2</sub>-Rich syngas from renewable sources by dual fluidized bed steam gasification of solid biomass. The 12th International Conference on Fluidization -New Horizons in Fluidization Engineering. 2007. Fluidization XII, 109.
- [61] Technologies relevant for gasification and methanation in Denmark: Detailed analysis of bio-SNG technologies and other RE-gases. 2012. [http://www.dgc.eu/sites/default/files/filarkiv/documents/R1207\\_gasification\\_methanisation.pdf](http://www.dgc.eu/sites/default/files/filarkiv/documents/R1207_gasification_methanisation.pdf) [Accessed 10.May.16] 736-50 Bio-SNG.
- [62] Schweitzer D, Beirrow M, Gredinger A, Armbrust N, Waizmann G, Dieter H, et al. Pilot-scale demonstration of oxy-SER steam gasification: production of syngas with pre-combustion CO<sub>2</sub> capture. *Energy Procedia* 2016;86:56–68.
- [63] Rostrup-Nielsen J. Catalysis science and technology. Berlin: Springer; 1984.
- [64] Williams R. Hydrogen production. 1933.
- [65] Hufton JR, Mayorga S, Siricar S. Sorption enhanced reaction process for hydrogen production. *AIChE J* 1999;45:248–56.
- [66] Wess R, Nores-Pondal F, Laborde M, Giunta P. Single stage H<sub>2</sub> production, purification and heat supply by means of Sorption-enhanced Steam Reforming of Glycerol. A thermodynamic analysis. *Chem Eng Sci* 2015;134:86–95.
- [67] Coefficients of calculating thermodynamics and transport properties of individual species. NASA report TM-4513. 1993. <https://ntrs.nasa.gov/archive/nasa/casi.ntrs.nasa.gov/19940013151.pdf> [Accessed 05.May.14].
- [68] Composition variety complicates processing plans for US shale gas. USA: Bryan Research & Engineering Inc; 2008. [www.digitalrefining.com/article/1000568](http://www.digitalrefining.com/article/1000568) [Accessed 21.February.17].
- [69] Mokhatab S, Poe WA. Handbook of natural gas transmission and processing. 2 ed. USA: Gulf Professional Publishing; 2012.
- [70] Sonibare JA, Akeredolu FA. A theoretical prediction of non-methane gaseous emissions from natural gas combustion. *Energy policy* 2004;32:1653–65.
- [71] Peebles MWH. Natural gas fundamentals. London: Shell International Gas Limited; 1992.
- [72] Florin NH, Harris AT. Hydrogen production from biomass coupled with carbon dioxide capture: the implications of thermodynamic equilibrium. *Int J Hydrogen Energy* 2007;32:4119–34.
- [73] Wei L, Xu S, Liu J, Liu C, Liu S. Hydrogen production in steam gasification of biomass with CaO as a CO<sub>2</sub> absorbent. *Energy Fuels* 2004;22:1997–2004.
- [74] Antzara A, Heracleous E, Bukur DB, Lemonidou AA. Thermodynamic analysis of hydrogen production via chemical looping steam methane reforming coupled with in situ CO<sub>2</sub> capture. *Energy Procedia* 2014;63:6576–89.
- [75] Laosiripojana N, Rajesh SK, Singhto W, Palikanon T, Pengyong S. Effects of H<sub>2</sub>S, CO<sub>2</sub>, and O<sub>2</sub> on catalytic methane steam reforming over Ni catalyst on CeO<sub>2</sub> and Al<sub>2</sub>O<sub>3</sub> supports. In: The joint international conference on “sustainable energy and environment (SEE)”. Hua Hin, Thailand; 2004.
- [76] Olsbye U, Wurzel T, Mleczko L. Kinetic and reaction engineering studies of dry reforming of methane over a Ni/La/Al<sub>2</sub>O<sub>3</sub> catalyst. *Ind Eng Chem Res* 1997;36:5180–8.
- [77] Barroso Quiroga MM, Castro Luna AE. Kinetic analysis of rate data for dry reforming of methane. *Ind Eng Chem Res* 2007;46:5265–70.